

# Polarizational colours could help polarization-dependent colour vision systems to discriminate between shiny and matt surfaces, but cannot unambiguously code surface orientation

Ramón Hegedüs, Gábor Horváth \*

*Biooptics Laboratory, Department of Biological Physics, Loránd Eötvös University, Pázmány Péter Sétány 1, H-1117 Budapest, Hungary*

Received 5 March 2004; received in revised form 30 April 2004

## Abstract

It was hypothesized that egg-laying *Papilio* butterflies could use polarizational colours as a cue to detect leaf orientation and to discriminate between shiny and matt leaves. These hypotheses would be supported if the following general questions were answered positively: (1) Can surface orientation be unambiguously coded by the polarizational colours perceived by polarization-sensitive colour vision systems? (2) Are the changes in the polarizational colours due to retinal rotation significantly different between shiny and matt surfaces? Using video polarimetry, we measured the reflection-polarizational characteristics of a shiny green hemisphere in the red, green and blue spectral ranges for different solar elevations and directions of view with respect to the solar azimuth as well as for sunlit and shady circumstances under clear skies. The continuously curving hemisphere models numerous differently oriented surfaces. Using the polarization- and colour-sensitive retina model developed earlier, we computed the polarizational colours of the hemisphere, and investigated the correlation between colours and local surface orientation. We also calculated the maximal changes of the polarizational colours of shiny and matt hemispheres induced by rotation of the retina. We found that a surface with any orientation can possess almost any polarizational colour under any illumination condition. Consequently, polarizational colours cannot unambiguously code surface orientation. Polarization sensitivity is even disadvantageous for the detection of surface orientation by means of colours. On the other hand, the colour changes due to retinal rotation can be significantly larger for shiny surfaces than for matt ones. Thus, polarizational colours could help discrimination between shiny and matt surfaces. The physical and perceptual reasons for these findings are explained in detail. Our results and conclusions are of general importance for polarization-dependent colour vision systems.

© 2004 Elsevier Ltd. All rights reserved.

**Keywords:** Polarization vision; Colour vision; Usefulness of polarizational colours; Surface orientation; Surface roughness

## 1. Introduction

Wehner and Bernard (1993) suggested that the combination of polarization and colour vision should be avoided, because the general consequence for visual systems is the occurrence of polarization-induced false colours if both qualities are mixed. They also proposed that the functional significance of the photoreceptor twist in honeybees is to avoid these polarizational colours of natural, bee-relevant surfaces (e.g. leaves and flower petals), which reflect partially linearly polarized light. The degree and angle of polarization of reflected

light depend on the roughness and orientation of plant surfaces (Horváth, Gál, Labhart, & Wehner, 2002). For a flower-visitor this could cause difficulties, because the photopigments responsible for colour vision are in receptors with different microvilli orientations. Thus, each receptor gives a signal that depends not only on intensity and wavelength but also on the angle and degree of polarization. If the receptors of a colour vision system are also polarization sensitive, the system generates false colours that may obscure the real colours determined by the spectral characteristics of objects and perceived by polarization-insensitive colour vision systems.

Thus, it was rather surprising when Kelber (1999) and Kelber, Thunell, and Arikawa (2001) demonstrated that *Papilio* butterflies perceive polarization-induced false colours under laboratory conditions, because the

\* Corresponding author.

E-mail address: [gh@arago.elte.hu](mailto:gh@arago.elte.hu) (G. Horváth).

photoreceptors of their colour vision system are weakly polarization sensitive. Since polarizational colours were believed to be disadvantageous and are generally eliminated in insect eyes by a proper twist of the photoreceptors (e.g. Wehner, Bernard, & Geiger, 1975), or by random microvilli orientations, or by monochromacy of the polarization-sensitive receptors (e.g. Wehner & Bernard, 1993), there should be some selective advantages to animals that have retained the polarization-dependence of their colour vision (Kelber, 1999; Kelber et al., 2001). For example, the females of *Papilio* butterflies lay eggs on the shiny leaves of plants in the Rutaceae or *Citrus* family. Kelber and her collaborators suggested that the polarizational colours perceived by these insects may be behaviourally relevant in the context of oviposition:

- (i) Kelber (1999) hypothesized that “horizontally oriented leaves would probably be more attractive than vertically oriented leaves to an ovipositing butterfly because they would provide a better landing for the butterfly and offer more protection for the eggs and young larvae”. The reflection-polarizational characteristics of plant surfaces depend strongly on their orientation, the illumination conditions and the direction of observation (Hegedüs & Horváth, in press; Horváth et al., 2002; Horváth & Varjú, 2003). According to Kelber et al. (2001, p. 2478), “to an approaching *Papilio* female, the shiny leaves of a *Citrus* bush should have different colours depending on their orientation: a horizontally oriented leaf should look more green whereas a vertically oriented leaf should look more blue–green or reddish. Horizontally oriented leaves should therefore be more attractive to an approaching female, whereas vertically oriented leaves should be less attractive. We do not know whether butterflies use the colour difference as a cue to detect leaf orientation, whether they prefer to lay eggs on horizontally oriented leaves and whether it is of advantage to lay eggs on horizontally oriented leaves”.
- (ii) Kelber (1999) also hypothesized that the detection of polarizational colours “may help butterflies to find optimal oviposition sites” and “could enable butterflies to discriminate between shiny and matt leaves before landing on them”. In her opinion, “leaves reflect different amounts of polarized light, so the colours of glossy and matt leaves should look different to a butterfly, and the colour should change when the butterfly passes by. This property might serve as an indicator of their quality as a food source for the caterpillar”. In the opinion of Kelber et al. (2001, p. 2478), “as a whole, a plant with shiny leaves should look more colourful than one that does not reflect polarized light. This could help the females to choose the larval food plant from a distance. The polariza-

tion-sensitive colour vision system could therefore be a ‘matched filter’ for optimal oviposition sites”.

These hypotheses raise the general questions:

- (1) Can the orientation of a surface be unambiguously coded by the polarizational colours perceived by polarization-dependent colour vision systems?
- (2) Are the changes in the polarizational colours due to retinal rotation significantly different between shiny and matt surfaces?

The aim of this work is to answer both general questions. Using video polarimetry, we measured the reflection-polarizational characteristics of a shiny green hemisphere in the red, green and blue spectral ranges under 60 different illumination conditions (for different solar elevations and directions of view with respect to the solar azimuth as well as for sunlit and shady circumstances) under clear sky. Since different points of the continuously curving surface of the hemisphere represent different surface orientations, the hemisphere models numerous differently oriented surfaces. Using the polarization- and colour-sensitive retina model of Horváth et al. (2002), we computed the polarizational colours of the hemisphere. We investigated the correlation between these colours and the local surface orientation of the hemisphere. We also calculated the maximal changes of the polarizational colours of shiny and matt hemispheres induced by retinal rotation. We found that a surface with any orientation can possess almost any polarizational colour under any illumination condition. Consequently, polarizational colours cannot unambiguously code surface orientation. In fact, depending on the microvilli directions, the polarization sensitivity of colour vision can even degrade the efficiency of detecting surface orientation by means of colours. On the other hand, the colour changes induced by retinal rotation can be significantly larger for shiny surfaces than for matt ones. Thus, polarizational colours could help discrimination between shiny and matt surfaces. Hence, question 1 is answered negatively, while question 2 positively. Our results and conclusions are of general importance for polarization-dependent colour vision systems; they are valid not only for the investigated special case of leaves, leaf orientation, *Papilio* retina and oviposition.

## 2. Materials and methods

### 2.1. Measurement of the reflection-polarization patterns of a shiny green hemisphere modelling numerous differently oriented surfaces

Our original aim was to measure the reflection-polarizational characteristics of a shiny green leaf blade

in the field for numerous different orientations  $\theta$ ,  $\varphi$  of its normal vector  $\underline{n}$  (Fig. 1A) at different solar elevations  $\varepsilon_S$  and directions of view  $\gamma$  with respect to the solar azimuth (Fig. 1C). However, at a given  $\varepsilon_S$  and  $\gamma$  the duration of the measurements with various  $\theta$ , and  $\varphi$

would have been so long that in the meantime the celestial polarization pattern as well as  $\varepsilon_S$  and  $\gamma$  would have changed considerably. Thus, we decided to use a shiny green hemisphere, the continuously curving surface of which models differently oriented shiny green

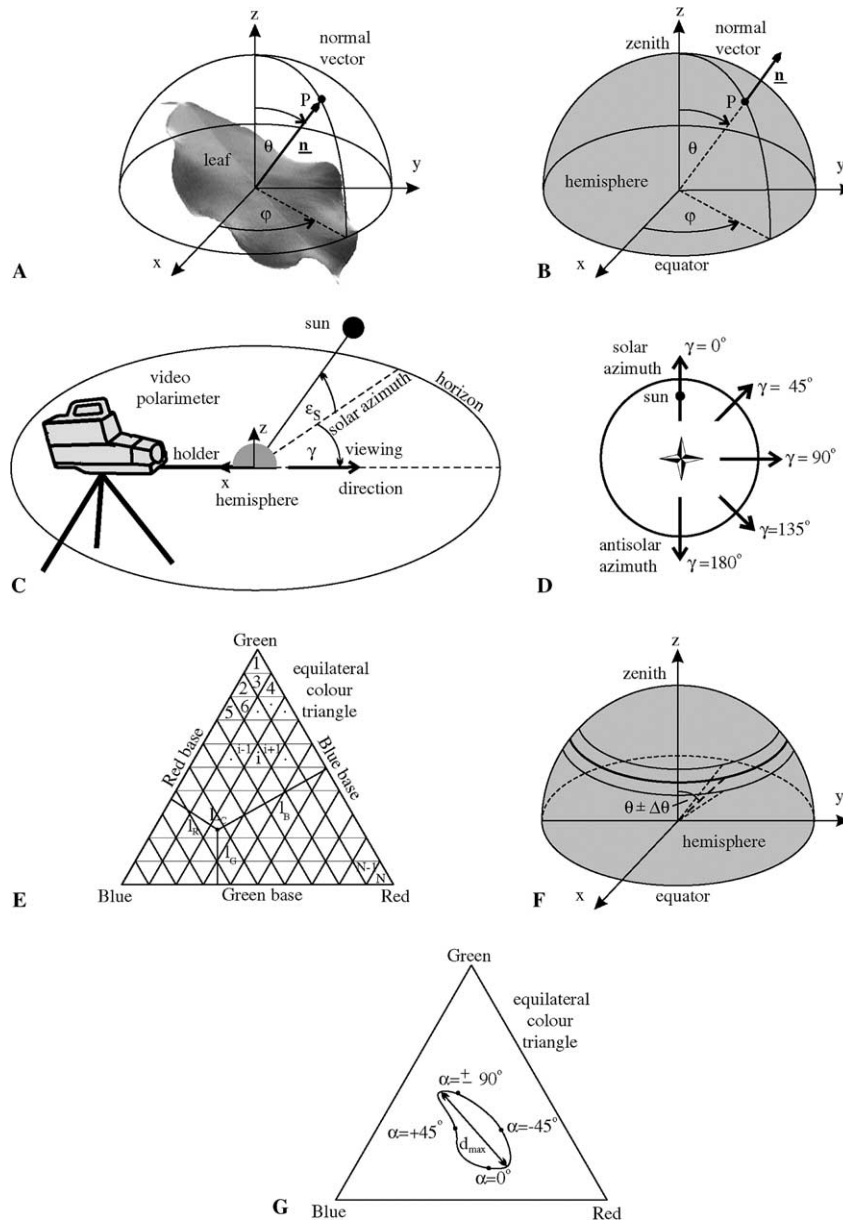


Fig. 1. (A) A leaf blade with a given orientation is described by the zenith angle  $\theta$  and azimuth angle  $\varphi$  of the normal vector  $\underline{n}$  of its surface. (B) A hemisphere, the surfacial points of which model numerous differently oriented (leaf) surfaces in the following ranges of  $\theta$  and  $\varphi$ :  $0^\circ \leq \theta \leq 90^\circ$ ,  $-90^\circ \leq \varphi \leq +90^\circ$ . (C) The arrangement of the measurement of the reflection-polarizational characteristics of the hemisphere at a given solar elevation  $\varepsilon_S$  and direction of view  $\gamma$  with respect to the solar azimuth. (D) Viewing directions  $\gamma$  of the polarimeter seen from above. (E) The three coordinates  $\ell_R, \ell_G$  and  $\ell_B$  of the spectral locus  $L_C$  ( $\ell_R, \ell_G, \ell_B$ ) of a perceived colour  $C$  is displayed in the equilateral, unit-sided Red–Green–Blue colour triangle, which is divided into  $N$  small triangles with an identity number  $n$  ranging from 1, 2, 3, ... through  $i - 1, i, i + 1, \dots$  to  $N - 1, N$ . (F) A band with an angular width of  $2 \times \Delta\theta$  on the hemisphere at zenith angle  $\theta$  (called the  $\theta$ -zone), representing a possible optimal zone (e.g. for butterfly egg-laying). (G) The locus of the polarizational colour of a point of the hemisphere moves along a closed loop in the equilateral colour triangle as the retina makes a half rotation, i.e. the angle  $\alpha$  of the eye's dorso-ventral meridian (measured from the vertical) changes from  $-90^\circ$  to  $+90^\circ$ . The maximal spectral distance  $d_{\max}$  between the points of this loop is the measure of the maximum difference in the polarizational colours due to retinal rotation. Four colour loci are shown for  $\alpha = \pm 90^\circ, -45^\circ, 0^\circ$  and  $+45^\circ$  along the loop, the dimensions of which are extremely enlarged for the sake of a better visualization.

(leaf) surfaces in the following ranges of  $\theta$  and  $\varphi$ :  $0^\circ \leq \theta \leq 90^\circ$ ,  $-90^\circ \leq \varphi \leq 90^\circ$  (Fig. 1B). The hemisphere was the upper half of a shiny green billiard ball with a diameter of 5 cm. The ball was fixed to a horizontal holder at a distance of 33 cm from the lens of the video camera of our imaging polarimeter in such a way that the horizontally oriented optical axis of the camera passed through the equator and the centre of the ball. The camera with the holder and ball could rotate around a vertical axis to ensure different viewing directions  $\gamma$  relative to the solar azimuth (Fig. 1C). The magnification of the camera optics was set in such a way that the upper half of the ball filled the entire field of view of the camera (Fig. 2).

Using video polarimetry, the patterns of the intensity  $I$ , degree of linear polarization  $\delta$  and angle of polarization  $\chi$  (measured from the vertical) of light reflected from the upper hemisphere of the billiard ball (Fig. 2) were measured in the blue (B), green (G) and red (R) spectral ranges at  $\lambda_B = 450 \pm 40$  nm (wavelength of maximal sensitivity  $\pm$  half bandwidth of the camera's CCD sensors),  $\lambda_G = 550 \pm 40$  nm and  $\lambda_R = 650 \pm 40$  nm under clear sky at solar elevations  $\varepsilon_S = 2^\circ, 11^\circ, 19^\circ, 26^\circ, 30^\circ, 32^\circ$  and viewing directions  $\gamma = 0^\circ, 45^\circ, 90^\circ, 135^\circ, 180^\circ$  from the solar azimuth (Fig. 1C and D). The method of video polarimetry is described in detail by Horváth and Varjú (1997). At a given  $\varepsilon_S$  and  $\gamma$ , two measurements were performed: (i) the ball was lit by direct sunlight and skylight ("sunlit" situation), or (ii) it was lit only by skylight, because the sun was occluded by a small disk ("shady" situation). Thus, the  $I$ -,  $\delta$ - and  $\chi$ -patterns of the hemisphere were measured in  $6(\varepsilon_S) \times 5(\gamma) \times 2$  (sunlit or shady) = 60 different illumination situations. The differently illuminated hemispheres are referred to as  $H_1, H_2, \dots, H_{60}$  further on.

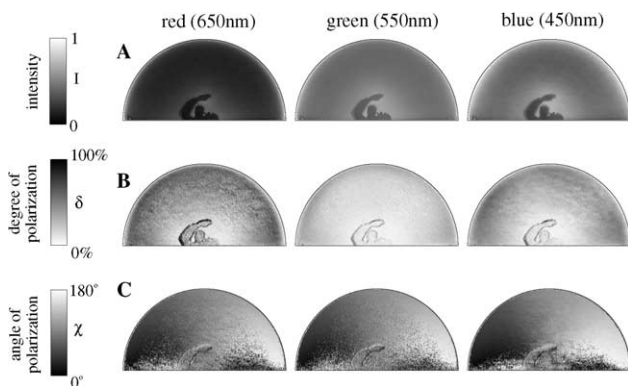


Fig. 2. Examples for the patterns of the intensity  $I$ , degree of linear polarization  $\delta$  and angle of polarization  $\chi$  (from the vertical) of the shiny green hemisphere measured by video polarimetry in the red, green and blue part of the spectrum under clear sky at solar elevation  $\varepsilon_S = 32^\circ$  and direction of view  $\gamma = 180^\circ$  relative to the solar azimuth. At the centre of the hemisphere the unavoidable mirror image of the polarimeter and its operator is seen. The operator occluded the sun behind him with his left hand in order to shade the hemisphere.

Since our hemisphere models not only differently oriented leaves, our studies can answer questions 1 and 2 quite generally, independently of the kind of surface (e.g. leaf, flower, spathe, petal, etc.).

## 2.2. Calculation of polarizational colours

The spectral loci of colours perceived by a polarization- and colour-sensitive insect retina—modelling, for example, the retina of *Papilio* butterflies—was calculated as described in detail by Horváth et al. (2002). Here we mention only that the quantum catches  $q_r$  of photoreceptors of spectral types  $r$  (= Red, Green, Blue) were calculated from the formula derived by Horváth et al. (2002) for integral normalization of the absorption functions  $A_r(\lambda)$  of receptors. The three coordinates  $\ell_R$ ,  $\ell_G$  and  $\ell_B$  of the spectral locus  $L_C(\ell_R, \ell_G, \ell_B)$  of the perceived colour  $C$  within the equilateral, unit-sided Red–Green–Blue colour triangle are (Fig. 1E):  $\ell_R = q_R/(q_R + q_G + q_B)$ ,  $\ell_G = q_G/(q_R + q_G + q_B)$ ,  $\ell_B = q_B/(q_R + q_G + q_B)$ . Note that  $\ell_R + \ell_G + \ell_B = 1$ .

The unit-sided colour triangle was divided into  $N$  small equilateral triangles with different identity numbers  $n$  ranging from 1, 2, 3, ... through  $i - 1, i, i + 1, \dots$  to  $N - 1, N$  (Fig. 1E). These small colour triangles represent  $N$  different colour regions in the unit-sided R–G–B colour space and determine the colour resolution of our investigations: each small triangle has sides with equal length of  $1/\sqrt{N}$  (since the side-length of the large colour triangle is 1), which can be considered as the minimum difference in colour that can be distinguished by our model retina. The absorption functions  $A_r(\lambda)$  of the R, G and B photoreceptors in our model retina were the same as those of *Papilio* butterflies (see Kelber et al., 2001; Horváth et al., 2002). The microvilli directions  $\beta_R, \beta_G$  and  $\beta_B$  measured from the eye's dorso-ventral meridian and the polarization sensitivity ratios  $P_R, P_G$  and  $P_B$  of the red, green and blue receptors were chosen according to the characteristics of the photoreceptors found by Kelber et al. (2001) in the butterfly *Papilio xuthus*.

Since at present the colour discrimination ability of *Papilio* butterflies is unknown, it was preferable to perform our investigations with the highest colour resolution possible. A higher colour resolution means a subtler colour discrimination. Thus, we used the maximal colour resolution achievable by our video polarimeter with 8 bit for every colour (R, G, B) channel. This technical limitation yields  $N = 640000$  for the number of the small colour triangles mentioned above.

## 2.3. Calculation of the probability of selection of optimal surface orientation by means of polarizational colours

According to the hypothesis of Kelber and collaborators, egg-laying *Papilio* butterflies may prefer such

shiny green leaves, the orientation of which falls within an (unknown) optimal interval  $\theta_{\text{opt}} \pm \Delta\theta$ , which could be advantageous to oviposition. In the context of oviposition only the tilt angle  $\theta$  of the leaf blade relative to the vertical (Fig. 1A and B) is important for a female butterfly which can approach the leaf from various azimuth directions  $\varphi$ . Therefore, consider a band with an angular width of  $2 \times \Delta\theta = 2 \times 3^\circ = 6^\circ$  at a given zenith angle  $\theta$  on the shiny green hemisphere (Fig. 1F). We call this area the “ $\theta$ -zone” modelling such (leaf) surfaces, the zenith angle of the normal vectors of which falls within the interval  $\theta \pm \Delta\theta$ . The  $\theta$ -zone at (unknown)  $\theta_{\text{opt}}$  is called the “optimal zone”, where points on the hemisphere falling within the interval  $\theta_{\text{opt}} \pm \Delta\theta$  represent optimally oriented (leaf) surfaces that are appropriate for egg-laying.

Given the identity number  $n$  of the small colour triangles and the zenith angle  $\theta$  on the hemisphere  $H_i$  ( $i = 1, 2, \dots, 60$ ) we define a matrix  $\underline{M}(H_i)$  called the “polarizational colour occurrence matrix”, the elements of which are  $M_{n,\theta}(H_i)$ . At the beginning  $M_{n,\theta}(H_i) = 0$  is set for all matrix elements. For all differently illuminated hemispheres  $H_i$  ( $i = 1, 2, \dots, 60$ ) we calculated the coordinates  $\ell_R, \ell_G, \ell_B$  of the spectral locus  $L_C(\ell_R, \ell_G, \ell_B)$  of the colour  $C$  perceived by the model retina at every point  $P$  on the hemisphere, and determined the identity number  $n$  of that small colour triangle in which  $C$  falls, as well as the zenith angle  $\theta_p$  of the normal vector of the point. The total investigated range (from  $0^\circ$  to  $90^\circ$ ) of the zenith angle  $\theta$  was divided into 30 intervals of uniform width of  $3^\circ$  and we determined the interval  $\theta \pm 1.5^\circ$ , in which  $\theta_p$  falls. Then, the corresponding element  $M_{n,\theta}(H_i)$  of matrix  $\underline{M}(H_i)$  was enhanced by 1. Thus, for every differently illuminated hemisphere  $H_i$  we obtained a colour occurrence matrix  $\underline{M}(H_i)$ , an element  $M_{n,\theta}(H_i)$  of which gives how many times a colour with identity number  $n$  occurs at the zone of points with zenith angle  $\theta \pm 1.5^\circ$  on hemisphere  $H_i$ . Finally, a net colour occurrence matrix  $\underline{M} = \sum_{i=1}^{60} \underline{M}(H_i)$  was calculated, which is the sum of matrices  $\underline{M}(H_i)$  belonging to the 60 different illumination situations. Since the extent of (and thus the number of points within) the  $\theta \pm 1.5^\circ$  zone diminishes with decreasing zenith angle  $\theta$ , the net colour occurrence matrix is normalized: its elements  $M_{n,\theta}$  are divided by the number of points in the  $\theta \pm 1.5^\circ$  zone. Note that the  $3^\circ$  resolution (i.e.  $\pm 1.5^\circ$ ) of zenith angle  $\theta$  in the colour occurrence matrices allows  $2 \times \Delta\theta = m \times 3^\circ$  values for the angular width of the optimal zone in the forthcoming calculations (see below), where  $m$  is a positive integer.

According to the hypothesis of Kelber and collaborators, the optimal (leaf) surface orientation  $\theta_{\text{opt}}$  may be unambiguously coded by the perceived polarizational colours. In our model, the points of the 60 hemispheres  $H_i$  ( $i = 1, 2, \dots, 60$ ) represent all the (leaf) surfaces occurring in the optical field of the model butterfly

looking for an optimally oriented (leaf) surface which is appropriate for oviposition, and the (leaf) surface orientation  $\theta$  is detected by the polarizational colours. As a working hypothesis let us assume that our model butterfly is able to memorize all polarizational colours occurring within the optimal zone of the hemispheres  $H_i$  ( $i = 1, 2, \dots, 60$ ). In other words, the butterfly must learn the identity numbers  $n_{\theta_{\text{opt}}}$  of all colours with  $M_{n,\theta} \neq 0$  in the net polarizational colour occurrence matrix  $\underline{M}$ , where  $\theta_{\text{opt}} - \Delta\theta < \theta < \theta_{\text{opt}} + \Delta\theta$ . The total number of points in the optimal zone of the hemisphere is  $N_{\theta_{\text{opt}}}^+ = \sum_n \sum_{\theta_{\text{opt}} - \Delta\theta < \theta < \theta_{\text{opt}} + \Delta\theta} M_{n,\theta}$ . After memorizing the optimal polarizational colours of these optimal points, the butterfly looks for such (leaf) surfaces (points on the hemisphere) as egg-laying sites, the polarizational colours of which are the same as one of the memorized optimal colours. However, some (leaf) surfaces (points on the hemisphere) can also possess optimal polarizational colours, the orientation of which is different from the optimal orientation, i.e. they are outside the optimal zone. Such (leaf) surfaces are inappropriately oriented for oviposition. Let the total number of the inappropriate points (leaves) on the hemisphere be  $N_{\theta_{\text{opt}}}^-$ . Then, the probability of egg-laying onto an optimally oriented (leaf) surface (points within the optimal zone on the hemisphere) is  $p(\theta_{\text{opt}}) = N_{\theta_{\text{opt}}}^+ / (N_{\theta_{\text{opt}}}^+ + N_{\theta_{\text{opt}}}^-)$ . Since  $\theta_{\text{opt}}$  is unknown, the probability  $p(\theta) = N_{\theta}^+ / (N_{\theta}^+ + N_{\theta}^-)$  is considered for any  $\theta$  values within the range from  $0^\circ$  to  $90^\circ$ , which is called the “probability of appropriate egg-laying” further on. At a given  $\theta$  the probability  $p(\theta)$  yields a value with the assumption that  $\theta \pm \Delta\theta$  is the optimal (leaf) surface orientation, implying that those polarizational colours are considered as optimal, which occur within the given  $\theta$ -zone. By definition of our model, if the butterfly is confronted with a (leaf) surface (point on the hemisphere), the polarizational colour of which is different from the memorized optimal colours, it does not select this (leaf) surface as an egg-laying site. If the butterfly selected randomly the oviposition site, the probability of egg-laying would be  $p^*(2 \times \Delta\theta = 6^\circ) = 6^\circ / 90^\circ = 1/15 \approx 0.067$ , when the angular width of the optimal zone on the hemisphere is  $2 \times \Delta\theta = 6^\circ$ .

In the investigation of the probability  $p(\theta)$  of appropriate egg-laying the colour discrimination ability of our model retina is crucial. We set the colour resolution  $N$  in the colour triangle to the maximal value (640 000) achievable by our video polarimeter. A representative estimation for the subtleness of the colour discrimination of our model retina corresponding to  $N = 640\,000$  can be obtained by determining the wavelength discrimination function  $\Delta\lambda(\lambda)$ , where  $\Delta\lambda$  is the minimal difference in wavelength that the retina can distinguish at wavelength  $\lambda$ , considering monochromatic light stimuli.  $\Delta\lambda(\lambda)$  was calculated with the assumption that the model retina is unable to detect colour differences smaller than  $1/\sqrt{N}$  (corresponding with the side

length of the small colour triangles in Fig. 1E) in the equilateral unit-sided colour triangle. This calculation showed that even at the worst wavelength discrimination,  $\Delta\lambda$  was not higher than about 1.6 nm, and for  $400 \text{ nm} < \lambda < 600 \text{ nm}$   $\Delta\lambda$  was smaller than 1 nm. These small  $\Delta\lambda$ -values represent an excellent colour discrimination ability. In honeybees, for example,  $\Delta\lambda_{\min} \approx 4 \text{ nm}$  (Neumeyer, 1991). Thus, using a colour resolution  $N = 640000$  for our model retina, we probably overestimate both the colour discrimination ability of *Papilio* butterflies and the probability  $p(\theta)$  of appropriate egg-laying.

#### 2.4. Calculation of the maximal change of polarizational colours of shiny and matt surfaces perceived by a rotating retina

Horváth et al. (2002) showed that the polarizational colours of surfaces perceived by a polarization- and colour-sensitive retina can more or less change as the retina rotates relative to the surface depending on its roughness. This phenomenon could be the basis of the visual discrimination between shiny and matt (leaf) surfaces (e.g. by egg-laying *Papilio* butterflies) as hypothesized earlier by Kelber and collaborators. In order to test this hypothesis, we calculated the polarizational colours of 60 differently illuminated shiny and matt hemispheres perceived by a weakly and a strongly polarization-sensitive retina (WPSR and SPSR) that was rotating. The locus  $L_C(\ell_R, \ell_G, \ell_B)$  of the polarizational colour  $C$  of every point on the hemispheres was displayed in the equilateral colour triangle as a function of the angle  $\alpha$  of the eye's dorso-ventral meridian measured from the vertical.  $L_C$  moves along a closed loop as the retina makes a half rotation, i.e.  $\alpha$  changes from  $-90^\circ$  to  $+90^\circ$  (Fig. 1G). We determined the maximal spectral distance  $d_{\max}$  between the points of this loop (Fig. 1G).  $d_{\max}$  is the measure of the maximum difference in the polarizational colour of a given point of the hemispheres due to retinal rotation. The mattness of the differently illuminated matt hemispheres was modelled in such a way that the degrees of linear polarization  $\delta$  of the differently illuminated shiny hemispheres  $H_i$  ( $i = 1, 2, \dots, 60$ ) were divided by 10:  $\delta_{\text{matt}} = \delta_{\text{shiny}}/10$ . The patterns of the intensity  $I$  and angle of polarization  $\chi$  were the same for both the shiny and matt hemispheres in a given illumination situation:  $I_{\text{matt}} = I_{\text{shiny}}$ ,  $\chi_{\text{matt}} = \chi_{\text{shiny}}$ .

### 3. Results

Fig. 2 shows examples for the patterns of the intensity  $I$ , degree of linear polarization  $\delta$  and angle of polarization  $\chi$  of light reflected from the shiny green hemisphere modelling numerous differently oriented surfaces. Although the hemisphere is green,  $I$  is relatively high

also in the blue, because the sun was occluded and the hemisphere was illuminated by the blue light from the clear sky in this particular case. The  $\delta$  of reflected light is lowest in the green, because the light reflected from the green subsurface layers is most intense in the green and thus it depolarizes most strongly the polarized light reflected from the surface (see Horváth et al., 2002). Fig. 2C demonstrates that the  $\chi$ -pattern of the hemisphere is practically independent of the wavelength  $\lambda$ , and due to the continuous curvature of the surface  $\chi$  changes widely within a given  $\theta$ -zone (e.g.  $\chi$  varies approximately from  $0^\circ$  to  $180^\circ$  for higher  $\theta$ ). Analysing the reflection-polarization patterns of the hemisphere measured under different illumination conditions, we established that the  $I$ -,  $\delta$ - and  $\chi$ -patterns of the hemisphere depend strongly on the solar elevation  $\varepsilon_s$  and the direction of view  $\gamma$  relative to the solar azimuth as well as on the presence of direct sunlight (sunlit or shady situation), due to the dependence of the skylight polarization on  $\varepsilon_s$  and  $\gamma$ . The  $I$ - and  $\delta$ -patterns depend greatly also on  $\lambda$ . The consequence of this is that the distribution of the polarizational colours on the hemisphere perceived by a polarization- and colour-sensitive retina depend also strongly on these variables.

Fig. 3 shows examples for the patterns of the polarizational colour difference  $\Delta\ell_{\text{green}} = |\ell_{\text{green}}^{\text{WPSR}} - \ell_{\text{green}}^{\text{PBR}}|$  between the components  $\ell_{\text{green}}^{\text{WPSR}}$  and  $\ell_{\text{green}}^{\text{PBR}}$  of colours of the hemisphere perceived by a weakly polarization-sensitive retina (WPSR) and a polarization-blind retina (PBR) with  $P_R = P_G = P_B = 1$  and  $\beta_R, \beta_G, \beta_B = \text{arbitrary}$  calculated for four different angles  $\alpha$  of the eye's dorso-ventral meridian. These patterns demonstrate how the polarizational colours differ from the real colours of the hemisphere perceived by a polarization-blind retina, and how these differences change as the retina rotates. These calculations were also made for the red and blue spectral ranges. The  $\Delta\ell_r$ -values ( $r = \text{red, green, blue}$ ) were smallest at  $\alpha = 90^\circ$  in the blue and largest at  $\alpha = 30^\circ$  in the green. Fig. 3 demonstrates well how the polarizational colours of a shiny green surface depend on its orientation (different points with different normal vectors on the hemisphere) as well as on the alignment  $\alpha$  of the eye's dorso-ventral meridian. Remember that one of the two general questions in this work is whether these polarizational colours can unambiguously code the surface orientation  $\theta$ .

Analyzing the (normalized) net polarizational colour occurrence matrix  $\underline{M} = \sum_{i=1}^{60} \underline{M}(H_i)$  (containing the number of occurrence of the polarizational colours at the interval of points with zenith angle  $\theta \pm 1.5^\circ$  on the hemisphere summed up for all 60 illumination situations as a function of  $\theta$ ), we found that at small zenith angles  $\theta$  only a few polarizational colours occur along a latitude due to the low number of points within the  $\theta$ -zone. As  $\theta$  increases, the number of polarizational colours in the  $\theta$ -zone increases suddenly, and it is saturated for

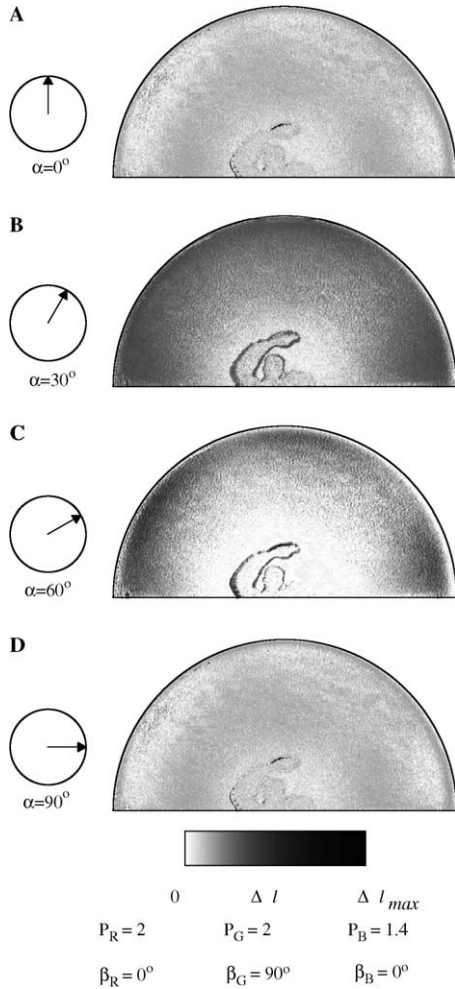


Fig. 3. Patterns of the difference  $\Delta \ell_{green} = |\ell_{green}^{WPSR} - \ell_{green}^{PBR}|$  between the components  $\ell_{green}^{WPSR}$  and  $\ell_{green}^{PBR}$  of colours of the shiny green hemisphere (the reflection-polarization patterns of which are shown in Fig. 2) perceived by a weakly polarization-sensitive retina (WPSR with polarization sensitivity ratios  $P_R = P_G = 2, P_B = 1.4$  and microvilli directions  $\beta_R = \beta_B = 0^\circ, \beta_G = 90^\circ$  measured from the dorso-ventral meridian of the eye) and a polarization-blind retina (PBR with  $P_R = P_G = P_B = 1$  and  $\beta_R, \beta_G, \beta_B =$  arbitrary) calculated for four different angles  $\alpha$  of the eye's dorso-ventral meridian measured from the vertical and displayed by the direction of a small arrow. The  $\Delta \ell_{green}$ -values are normalized to the maximal difference  $\Delta \ell_{max}$  (shaded by black) obtained throughout all the four difference patterns. Grey shades represent those points of the hemisphere, the perceived polarizational colour of which differs from the real green colour, while white represents the points, the perceived colour of which is the same as the real colour. At the centre of the hemisphere the unavoidable mirror image of the polarimeter and its operator is seen. The operator occluded the sun behind him with his left hand in order to shade the hemisphere.

higher  $\theta$ . Due to this saturation, if  $\theta > \theta^* = 15^\circ$ , practically every polarizational colour occurs several times within the  $\theta$ -zone, independently of  $\theta$ . This phenomenon casts the shadow before that the polarizational colours cannot code unambiguously the surface orientation  $\theta$ .

This prediction is proven in Fig. 4 in which the probability  $p(\theta)$  of appropriate egg-laying (definition see

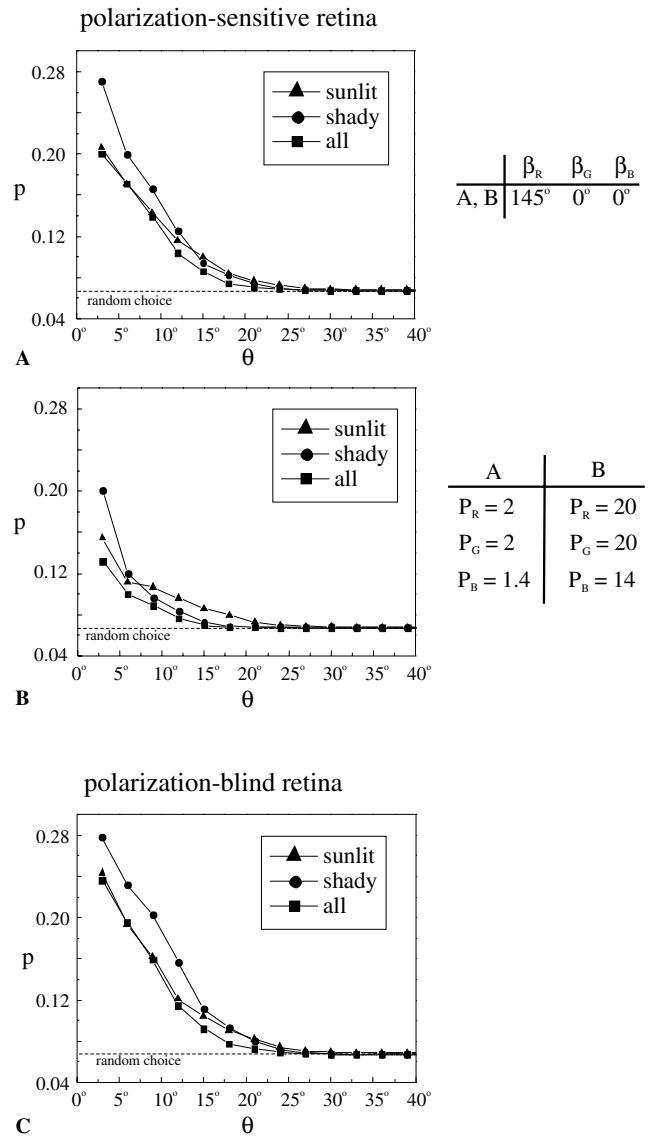


Fig. 4. (A,B) The probability  $p(\theta)$  of appropriate egg-laying as a function of the zenith angle  $\theta$  of the  $\theta$ -zone of width  $2 \times \Delta \theta = 6^\circ$  on the differently illuminated hemisphere modelling numerous differently oriented shiny green (leaf) surfaces.  $p(\theta)$  is calculated for a weakly (with polarization sensitivities  $P_R = P_G = 2, P_B = 1.4$ ) and a strongly (with  $P_R = P_G = 20, P_B = 14$ ) polarization-sensitive retina (WPSR and SPSR) with a given configuration of the microvilli directions  $\beta_R = 145^\circ, \beta_G = \beta_B = 0^\circ$  of the red, green and blue receptors measured from the eye's dorso-ventral meridian.  $p(\theta)$  is separately calculated for three different cases: (i) only for the 30 sunlit hemispheres (triangles), (ii) only for the 30 shady hemispheres (dots), (iii) for all 60 sunlit and shady hemispheres (squares). If the model butterfly selected randomly the oviposition site,  $p^* \approx 0.067$  which is displayed by a horizontal dashed line in the diagrams. Here  $p(\theta)$  is represented only in the interval  $0^\circ \leq \theta \leq 40^\circ$ , because  $p(\theta) = p^*$  for  $40^\circ < \theta \leq 90^\circ$  under all conditions. (C) As (A) and (B) for a polarization-blind retina (PBR) with  $P_R = P_G = P_B = 1$  and  $\beta_R, \beta_G, \beta_B =$  arbitrary.

in Section 2.3) is shown as a function of the zenith angle  $\theta$  of the  $\theta$ -zone of width  $2 \times \Delta \theta = 6^\circ$  on the hemisphere.  $p(\theta)$  gives the probability of egg-laying onto an optimally oriented leaf selected by means of the perceived

polarizational colour, assuming that  $\theta \pm \Delta\theta$  is the optimal orientation (i.e. that the  $\theta$ -zone is the optimal zone).  $p(\theta)$  was calculated for both WPSR and SPSR for six different configurations of the microvilli directions  $\beta_R, \beta_G$  and  $\beta_B$  occurring in *Papilio* butterflies. We obtained practically the same results as in Fig. 4A and B. The prerequisite of an unambiguous code of  $\theta$  by means of the polarizational colours is that  $p(\theta)$  must approximate 1. However, in Fig. 4 we can see that if  $\theta > \theta^* = 15^\circ$ ,  $p(\theta)$  is as low as  $p^* \approx 0.067$  for both the investigated weakly and strongly polarization-sensitive retinas (WPSR and SPSR) as well as for the polarization-blind retina (PBR), independently of the microvilli directions  $\beta_R, \beta_G, \beta_B$  of the red, green and blue receptors and whether the hemisphere is sunlit or shady. Note that  $p^* \approx 0.067$  is the probability of random choice.  $p(\theta)$  is usually slightly higher for shady hemispheres than for sunlit ones. For  $0^\circ \leq \theta \leq 15^\circ$  the probability  $p$  of appropriate egg-laying is larger than  $p^*$ , the maximum  $p$ -values range between 0.1 and 0.28. These relatively high  $p$ -values are the consequence of the fact that if  $\theta < \theta^* = 15^\circ$ , only a few polarizational colours occur in the  $\theta$ -zone due to its shortness. From this we conclude

that polarizational colours cannot unambiguously code the surface orientation  $\theta$ , if  $\theta > \theta^* = 15^\circ$ . Interestingly, for the PBR  $p(\theta)$  is usually higher (Fig. 4C) than for the WPSR and SPSR (Fig. 4A and B). Hence, polarization sensitivity is rather disadvantageous for detection of the surface orientation by means of colours.

Fig. 5 shows examples for the frequencies of the maximum spectral differences  $d_{\max}$  in the polarizational colours of shiny and matt hemispheres due to the rotation of a WPSR. These were also calculated for several microvilli directions  $\beta_R, \beta_G, \beta_B$  as well as for a SPSR (with  $P_R = P_G = 20, P_B = 14$ ). For the SPSR the  $d_{\max}$ -values were about 3 times larger than for the WPSR. Furthermore, we obtained that the averages  $\langle d_{\max} \rangle$  of the maximum spectral differences at the shiny hemispheres are about 10 times higher than those at the matt hemispheres for both the WPSR and SPSR, independently of  $\beta_R, \beta_G, \beta_B$  and whether the hemisphere is sunlit or shady. Note that  $\langle d_{\max} \rangle$  is always slightly higher at the shady than at the sunlit hemisphere for both the shiny and matt surfaces. Hence, the matter the surface, the smaller the differences in the polarizational colours induced by retinal rotation. From this we conclude that the change

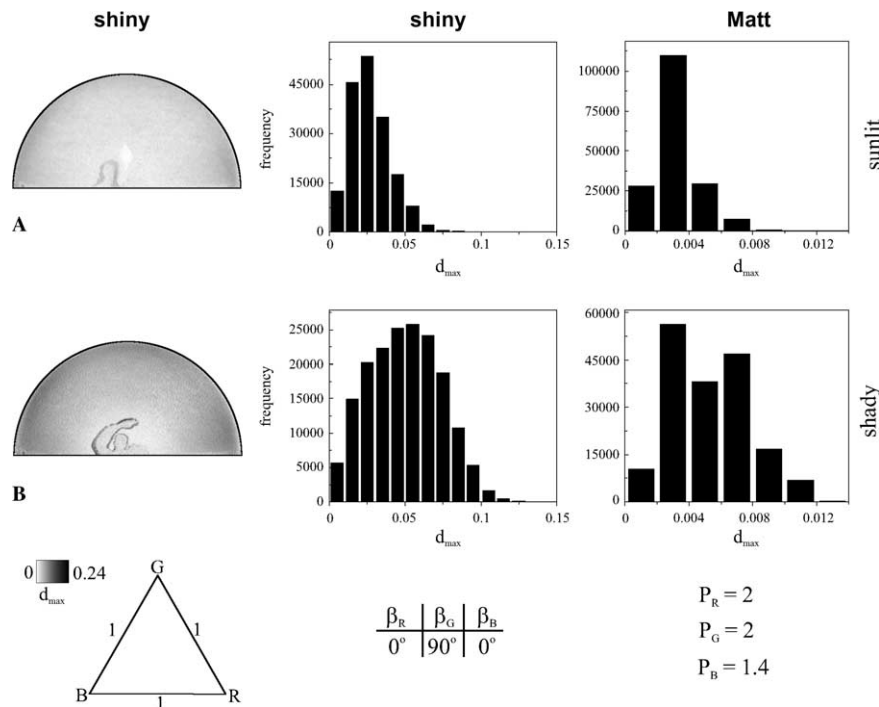


Fig. 5. Middle and right columns: Frequencies of the maximum differences  $d_{\max}$  in the polarizational colours of the differently illuminated shiny (middle column) and matt (right column) hemispheres due to the half rotation (the angle  $\alpha$  of the eye's dorso-ventral meridian measured from the vertical changes from  $-90^\circ$  to  $+90^\circ$ ) of a weakly polarization-sensitive retina (WPSR) with polarization sensitivity ratios  $P_R = P_G = 2, P_B = 1.4$  calculated for the sunlit and shady situations for a given configuration of the microvilli directions  $\beta_R = \beta_B = 0^\circ, \beta_G = 90^\circ$  of the red, green and blue receptors measured from the eye's dorso-ventral meridian. The mattness of the hemispheres was modelled in such a way that the degrees of linear polarization  $\delta$  of the shiny hemispheres were divided by 10:  $\delta_{\text{matt}} = \delta_{\text{shiny}}/10$ . The patterns of the intensity  $I$  and the angle of polarization  $\chi$  were the same for both the shiny and matt hemispheres under a given illumination condition:  $I_{\text{matt}} = I_{\text{shiny}}, \chi_{\text{matt}} = \chi_{\text{shiny}}$ . Left column: The distribution of  $d_{\max}$  on the shiny hemisphere, the reflection-polarization patterns of which are shown in Fig. 2. The  $d_{\max}$ -values are coded by different grey shades and are normalized in such a way that the side-length of the equilateral colour triangle is taken as 1 (Fig. 1G). The minimum (white) and maximum (black) of  $d_{\max}$  is 0 and 0.24, respectively.



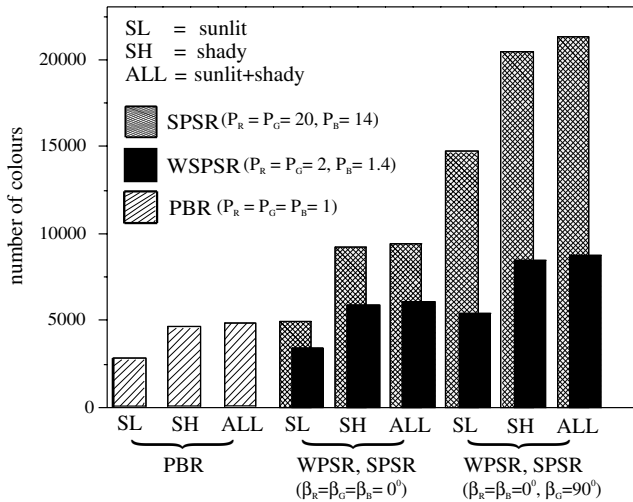


Fig. 6. The total number  $N_{total}$  of polarizational colours occurring on the 60 differently illuminated green hemispheres calculated for a weakly and a strongly polarization-sensitive retina (WPSR with  $P_R = P_G = 2, P_B = 1.4$  and SPSR with  $P_R = P_G = 20, P_B = 14$ ) with two different sets of the microvilli directions ( $\beta_R = \beta_G = \beta_B = 0^\circ$  and  $\beta_R = \beta_B = 0^\circ, \beta_G = 90^\circ$ ) as well as for a polarization-blind retina (PBR with  $P_R = P_G = P_B = 1; \beta_R, \beta_G, \beta_B = \text{arbitrary}$ ).  $N_{total}$  is separately calculated for three different cases: (i) only for the 30 sunlit hemispheres (SL), (ii) only for the 30 shady hemispheres (SH), (iii) for all 60 sunlit and shady hemispheres (ALL).

of polarizational colours due to retinal rotation could help discrimination between shiny and matt surfaces.

Fig. 6 shows the total number  $N_{total}$  of polarizational colours occurring on the 60 differently illuminated shiny green hemispheres calculated for the WPSR and SPSR as well as for the PBR.  $N_{total}$  is calculated for three different cases: (i) only for the 30 sunlit hemispheres, (ii) only for the 30 shady hemispheres, (iii) for all 60 sunlit and shady hemispheres. In Fig. 6 we can see that  $N_{total}$  is higher for the shady than for the sunlit situation;  $N_{total}$  is smaller for the PBR than for polarization-sensitive ones; and  $N_{total}$  is significantly greater for the SPSR than for the WPSR. We have seen above that the probability  $p(\theta)$  is usually higher for shady surfaces than for sunlit ones, while for the PBR  $p(\theta)$  is higher than for the WPSR and SPSR. This demonstrates that there is no direct correlation between  $N_{total}$  and  $p(\theta)$ , that is, a higher diversity of polarizational colours of surfaces (at all illumination situations and for all surface orientations) does not necessarily promote a more unambiguous coding of orientation  $\theta$ .

Fig. 7 shows the probability  $p(\theta)$  under shady circumstances as a function of the zenith angle  $\theta$  of the  $\theta$ -zone of width  $2 \times \Delta\theta$  on the hemisphere for different values of  $2 \times \Delta\theta$  ranging from  $6^\circ$  to  $30^\circ$  calculated for a WPSR. The horizontal dashed lines represent the probabilities  $p^*(2 \times \Delta\theta)$  of random choice. Similar results were obtained also for both the WPSR and SPSR with other sets of the microvilli directions  $\beta_R, \beta_G, \beta_B$  as well as for other illumination situations of the hemi-

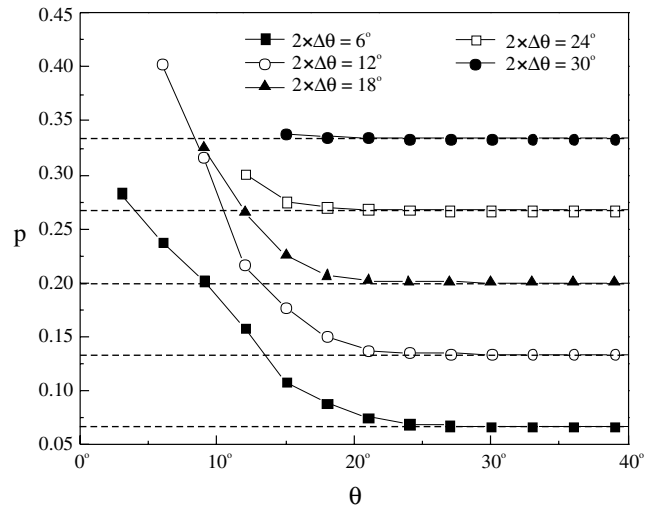


Fig. 7. The probability  $p(\theta)$  of appropriate egg-laying under shady circumstances as a function of the zenith angle  $\theta$  of the  $\theta$ -zone of width  $2 \times \Delta\theta$  on the hemisphere modelling numerous differently oriented shiny green (leaf) surfaces for different values of  $2 \times \Delta\theta$  ranging from  $6^\circ$  to  $30^\circ$ .  $p(\theta)$  is calculated for a weakly polarization-sensitive retina (WPSR) with  $P_R = P_G = 2, P_B = 1.4$  and microvilli directions  $\beta_R = \beta_G = \beta_B = 0^\circ$  of the red, green and blue receptors measured from the eye's dorso-ventral meridian. The horizontal dashed lines represent the probabilities  $p^*(2 \times \Delta\theta)$  of random choice, that is when the butterfly selects randomly the oviposition site.

sphere. We can see that as  $\Delta\theta$  increases,  $p(\theta)$  and  $p^*(2 \times \Delta\theta)$  increase and the difference  $\Delta p = p_{max} - p^*(2 \times \Delta\theta)$  decreases. Since considering the choice of appropriately oriented surfaces by means of colours the higher values of  $\Delta p$  are of relevance, we conclude that widening the  $\theta$ -zone on the hemisphere (i.e. increasing  $\Delta\theta$ ) reduces the chance of an unambiguous colour coding of the surface orientation  $\theta$ .

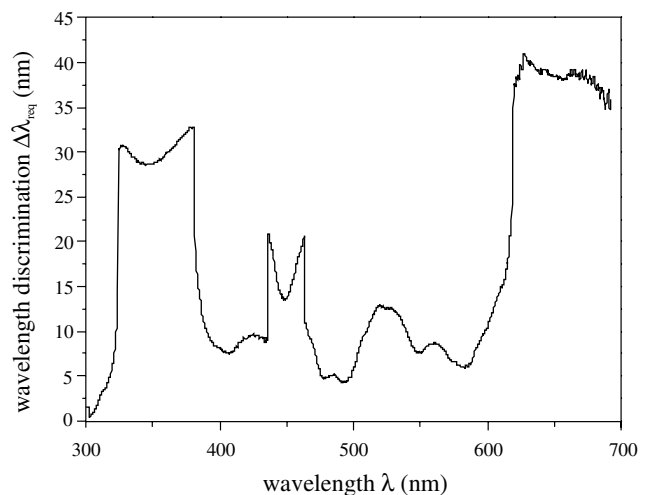


Fig. 8. The minimal wavelength discrimination ability  $\Delta\lambda_{req}(\lambda)$  required to perceive the colour differences  $d_{max} \geq 0.06$ , where the unit is the side length of the colour triangle.

Fig. 8 shows the minimal wavelength discrimination ability  $\Delta\lambda_{\text{req}}(\lambda)$  required to perceive the colour differences  $d_{\text{max}}$  in Fig. 5B by our model retina versus the wavelength  $\lambda$ .  $\Delta\lambda_{\text{req}}(\lambda)$  was calculated with the assumption that the model retina can perceive colour differences  $d_{\text{max}} \geq 0.06$ , where the unit is the side length of the colour triangle.

#### 4. Discussion

In this work we investigated the usefulness of polarizational colours in two visual tasks: (i) discrimination between surfaces of different roughness (shiny or matt), (ii) unambiguous colour coding of surface orientation. These tasks can be of general importance for polarization-dependent colour vision systems. Until now only in *Papilio* butterflies has been demonstrated behaviourally the occurrence of polarization-dependent colour vision. This is the reason why we studied the usefulness of polarizational colours in context of the egg-laying of these butterflies. However, our results and conclusions are quite general; they are valid not only for the special case of leaves, leaf orientation, *Papilio* retina and oviposition: For instance, in our study the “optimal zone” (i.e. the  $\theta$ -zone at  $\theta_{\text{opt}}$ , where points on the hemisphere fall within the interval  $\theta_{\text{opt}} \pm \Delta\theta$ ) represents not only optimally oriented leaves being appropriate for egg-laying, but more generally any optimally oriented surfaces which are appropriate for a particular task requiring the selection of (preferred, optimal) surface orientation. Similarly, the calculated “probability  $p(\theta)$  of appropriate egg-laying” can be generalized as the probability of selection of an appropriate (optimal) surface orientation. Although the polarizational colours perceived by our generalized polarization-sensitive model retina were computed for the particular parameters of the *Papilio* retina, our results remain generally valid for any polarization-dependent colour vision systems, because they are qualitatively independent of the microvilli directions, polarization sensitivities and absorption functions of the photoreceptors. Furthermore, our billiard ball models any green surfaces with different orientations. The particular colour of the billiard ball is of no importance, because the same conclusions could have been drawn for any other colours.

In nature, there are plenty of different leaf types with different spectral characteristics and surface roughness. The most frequent leaves are green with smooth surfaces, thus we used a shiny and (for the human eye) leaf-green hemisphere as a leaf model. The major advantage of this hemisphere is that the direction of the normal vector of its surface changes continuously within a wide range, modelling all possible leaf orientations (Fig. 1A and B). Thus, using imaging polarimetry, we could measure simultaneously the reflection-polarizational

characteristics of the leaf model at numerous different surface orientations under a given illumination condition (Fig. 2). Our approach, using an artificial green surface as a leaf imitation instead of a real leaf, is similar to that of Kelber (1999) and Kelber et al. (2001), who used also artificial surfaces as leaf-dummies in their behavioural experiments studying the polarization sensitivity of colour vision in *Papilio* butterflies.

The reflection-polarization patterns of our hemisphere are determined by the polarization pattern of the sky and the polarizing capability of the reflecting shiny green billiard ball. Since the celestial polarization pattern depends strongly on the solar elevation and the direction of view relative to the solar azimuth, the reflection-polarization pattern of the hemisphere changes significantly as these variables change. The reflection-polarizational characteristics of the hemisphere depend also on the presence of direct solar illumination: If the hemisphere is in shadow (because the direct sunlight is occluded), it is illuminated exclusively by linearly polarized blue skylight from all directions. If the sun is not occluded, a further component of the illumination is the monodirectional intense and unpolarized sunlight, the spectral characteristics of which are quite different from those of the skylight.

In our polarimetric measurements we used a shiny green billiard ball as a leaf model. In order to compare the reflection-polarizational characteristics of shiny and matt balls, we tried to make matt the surface of the ball either by sand-blowing or by chemical corrosion. However, by these methods we could not ensure a homogeneous surface roughness of the ball. Furthermore, if a shiny surface is made matt, not only the degree of linear polarization  $\delta$ , but also the intensity  $I$  and the angle of polarization  $\chi$  of reflected light can change. Thus we decided to model the mattness of the hemisphere by decreasing the measured  $\delta$ -values by a factor of 10. This approach is sound, because considering polarization, the most relevant difference between shiny and matt surfaces with the same spectral features is that rough surfaces polarize light much less than shiny surfaces. Another advantage of this approach is that the  $I$ - and  $\chi$ -patterns were the same for both the shiny and the simulated matt hemispheres. This is important, because we wanted to compare the rotation-induced changes  $d_{\text{max}}$  in the polarizational colours of hemispheres with the same brightness/colour and angle of polarization, but with different degrees of polarization, otherwise it would be unknown whether any difference in  $d_{\text{max}}$  between the shiny and matt surfaces is due to the differences in  $I$  and/or  $\chi$  and/or  $\delta$ .

The polarizational colours of our hemisphere (Fig. 3) calculated on the basis of the trichromatic retina model developed by Horváth et al. (2002) are determined by the reflection-polarizational characteristics of the billiard ball and the parameters of the retina. The

parameters of our WPSR are the same as those of the *Papilio* butterflies. Kelber et al. (2001) have shown that although *Papilio xuthus* and *P. aegeus* have a pentachromatic colour vision system, the behavioural data obtained for these species can be well explained also with the assumption of a trichromatic system. Similarly, Horváth et al. (2002) also showed the validity of their trichromatic retina model developed to describe the polarization- and colour-sensitive retina of *Papilio* butterflies.

In this work we showed that the change in the polarizational colours due to retinal rotation (Fig. 3) is significantly larger for shiny surfaces than for matt ones. This could help polarization-dependent colour vision systems to discriminate visually between shiny and matt surfaces from a distance. Such a rotation of the retina certainly occurs when an insect approaches a surface on wing, for instance. Another way of movement of the image of surfaces relative to the retina occurs when the animal passes by. The perceived polarizational colours change also strongly during such a translation (not demonstrated here), because the reflection-polarizational patterns of surfaces change significantly as the direction of view changes (e.g. Horváth et al., 2002; Horváth & Varjú, 2003). Thus, our conclusion, that the change of polarizational colours due to retinal rotation could help discrimination between shiny and matt surfaces, can be extended also to retinal translations.

We obtained that the polarizational colour differences  $d_{\max}$  due to retinal rotation (Fig. 5) are larger if the polarization sensitivities  $P_R, P_G, P_B$  of the receptors are higher. Furthermore these differences are greater for the retinas (both WPSR and SPSR) with microvilli directions  $\beta_R = \beta_B = 0^\circ, \beta_G = 90^\circ$  (Fig. 5) than for retinas with other microvilli orientations. However, since the colour discrimination ability of *Papilio* butterflies is unknown, at present it is unpredictable whether these colour differences  $d_{\max}$  are large enough to be perceived by these animals. Nevertheless, according to Fig. 8, the minimal colour discrimination ability is  $4 \text{ nm} < \Delta\lambda_{\text{req}}(\lambda) < 12 \text{ nm}$  which is required to perceive colour differences  $d_{\max} \geq 0.06$  in the green part of the spectrum, where the unit is the side length of the colour triangle. This means that if the colour discrimination ability of *Papilio* butterflies were in the range of that of honeybees (Neumeyer, 1991), these butterflies could probably perceive the polarizational colour differences due to retinal rotation, thus enabling them a possible way of visual discrimination between shiny and matt surfaces.

It is unknown whether butterflies prefer any leaf orientation for egg-laying and whether there is any advantage to lay eggs on particularly oriented leaves. Nevertheless, it is logical to assume that there is an optimal interval for the leaf orientation  $\theta$  (see Fig. 1A): If  $\theta \approx 0^\circ$  (approximately horizontal leaf blade), the leaf

could protect well the eggs (laid onto the back side) and the young larvae (feeding on the back side) against rain and sunshine, furthermore it could provide a better landing for the ovipositing butterfly, but the eggs and larvae could be easily detected from below by a predator. Hence, considering oviposition, nearly horizontally oriented leaves might be suboptimal.

In Fig. 4 we can see that for  $\theta > 15^\circ$  the probability  $p(\theta)$  is practically the same as that of random choice ( $p^* \approx 0.067$ ). Hence, the polarizational colours cannot unambiguously code the surface orientation  $\theta$  if the tiltiness of the surface is larger than  $15^\circ$  from the horizontal. In principle, polarizational colours could be used as a cue to detect the orientation of (leaf) surfaces, the tiltiness of which is smaller than  $15^\circ$  with respect to the horizontal. However, we have seen above that such, approximately horizontal (leaf) orientations may be suboptimal, considering oviposition, and on the other hand, detecting the (leaf) orientation by means of the polarizational colours with an error of 72–90% (due to  $0.1 \leq p(\theta) \leq 0.28$ ) can be considered rather insufficient.

In Fig. 4 we can see that the probability  $p(\theta)$  is highest at  $\theta < 15^\circ$  for both the WPSR and SPSR as well as for the PBR, independently of the microvilli directions. At  $\beta_R = \beta_G = \beta_B = 0^\circ$ ,  $p(\theta)$  has practically the same values for all three model retinas (WPSR, SPSR, PBR), while for other microvilli directions of the WPSR and SPSR we obtained (sometimes significantly) lower  $p(\theta < 15^\circ)$ -values than for the PBR.  $\beta_R = \beta_G = \beta_B = 0^\circ$  with the actually similar relative  $P_r$ -values ( $P_R = P_G = 2, P_B = 1.4$  for the WPSR;  $P_R = P_G = 20, P_B = 14$  for the SPSR) represent a quasi uniformly polarization-sensitive retina (UPSR), which has uniformly oriented microvilli with equal polarization sensitivities. Under natural conditions a UPSR often perceives only very weak polarization-induced false colours. If both the degree  $\delta$  and the angle  $\chi$  of polarization of the perceived light is wavelength-independent, a UPSR perceives the same colours as a PBR (Hegedüs & Horváth, in press). This explains why we obtained nearly the same  $p(\theta)$  functions for  $\beta_R = \beta_G = \beta_B = 0^\circ$  compared to  $p(\theta)$  of the PBR (Fig. 4C).

But even if there is a higher chance of selection of appropriate surface orientation than random choice for  $\theta < 15^\circ$ , since the highest probabilities  $p(\theta)$  are obtained for the PBR, we conclude that polarizational colours cannot make easier the finding of optimally oriented surfaces compared to the real colours perceived by a polarization-blind colour vision system. In fact, for many sets of the microvilli directions polarization sensitivity of the colour vision can even degrade the efficiency of detecting appropriate surface orientations by means of colours.

Since higher polarization sensitivity (PS) results in greater shifts of the perceived colours relative to the real

ones (perceived by a PBR), the visual world of a SPSR is more colourful than that of a WPSR (Horváth et al., 2002). Thus, one could expect that the more diverse (i.e. numerous) colours of surfaces perceived by a SPSR and demonstrated in Fig. 6 could enable a more unambiguous colour coding of the surface orientation than for a WPSR. However, at a given set of the microvilli directions  $\beta_R$ ,  $\beta_G$  and  $\beta_B$  there were no significant differences in  $p(\theta)$  between the WPSR and SPSR (Fig. 4). The reason for this is that at a given  $\theta$  there is hardly any constancy in the degree  $\delta$  and angle  $\chi$  of polarization, in particular  $\chi$  changes practically over the entire spectrum of its possible values (Fig. 2). Consequently, regardless of PS resulting in higher or smaller number of distinguishable colours within a given  $\theta$ -zone ( $\theta \pm \Delta\theta$ ) on the spectrally uniformly green hemisphere, approximately the same polarizational colours occur always within each zone almost independently of  $\theta$  due to the high variance in  $\delta$  and  $\chi$ , especially for larger  $\theta$  values. In other words, a surface with any orientation can possess almost any polarizational colour under any illumination condition. This phenomenon hinders an unambiguous colour coding of surfaces with different orientation  $\theta$ .

Another counter-argument against detecting the surface orientation by means of polarizational colours is that an animal should memorize too many different colours which code the optimal surface orientations (Fig. 6). It is questionable whether butterflies are able to memorize so many different colours and can learn the association between these colours and the optimal surface orientations (if any).

Based on the above findings, we can draw the general conclusion that polarizational colours (which tend to obscure the real colours rather randomly due to the random temporal and/or spatial changes of the degree and angle of polarization along surfaces) are useless for polarization-dependent colour vision systems to identify a particular/preferred surface orientation (e.g. for butterflies to find optimally oriented leaves for oviposition). In fact, the lack of unambiguous correlation between colours and surface orientations renders the identification of surface orientation much more difficult than it is for a polarization-blind colour vision system. A possible advantage polarization-dependent colour vision systems could gain is the detection of the magnitude of changes

in polarizational colours due to retinal rotation/translation, since these changes are primarily determined by the surface roughness and are not subject to further major temporal or spatial ambiguities.

### Acknowledgements

This work was supported by a three-year István Széchenyi scholarship from the Hungarian Ministry of Education to Gábor Horváth. Many thanks are due to two anonymous reviewers for their constructive comments. We are grateful to Sandor Hopp (Mechanical Workshop of the Eotvos University) for constructing the holder of the camera and the billiard ball.

### References

- Hegedüs, R., & Horváth, G., (in press). How and why are uniformly polarization-sensitive retinæ subject to polarization-related artefacts? Correction of some errors in the theory of polarization-induced false colours. *Journal of Theoretical Biology*.
- Horváth, G., Gál, J., Labhart, T., & Wehner, R. (2002). Does reflection polarization by plants influence colour perception in insects? Polarimetric measurements applied to a polarization-sensitive model retina of *Papilio* butterflies. *Journal of Experimental Biology*, 205, 3281–3298.
- Horváth, G., & Varjú, D. (1997). Polarization pattern of freshwater habitats recorded by video polarimetry in red, green and blue spectral ranges and its relevance for water detection by aquatic insects. *Journal of Experimental Biology*, 200, 1155–1163.
- Horváth, G., & Varjú, D. (2003). *Polarized light in animal vision—polarization patterns in nature*. Heidelberg, Berlin, New York: Springer-Verlag.
- Kelber, A. (1999). Why 'false' colours are seen by butterflies. *Nature*, 402, 251.
- Kelber, A., Thunell, C., & Arikawa, K. (2001). Polarisation-dependent colour vision in *Papilio* butterflies. *Journal of Experimental Biology*, 204, 2469–2480.
- Neumeyer, C. (1991). Evolution of colour vision. In J. R. Cronly-Dillon & R. L. Gregory (Eds.), *Evolution of the eye and visual system: Vol. 2. Vision and visual dysfunction* (pp. 285–305). London: MacMillan Press.
- Wehner, R., & Bernard, G. D. (1993). Photoreceptor twist: a solution to the false-color problem. *Proceedings of the National Academy of Sciences of the USA*, 90, 4132–4135.
- Wehner, R., Bernard, G. D., & Geiger, E. (1975). Twisted and non-twisted rhabdoms and their significance for polarization detection in the bee. *Journal of Comparative Physiology*, 104, 225–245.